Simulation of Steel Armour Penetration Using the Johnson−Cook Model[*]

Adam WIŚNIEWSKI, Łukasz TOMASZEWSKI

Military Institute of Armament Technology,
7 Wyszyńskiego St., 05-220 Zielonka, Poland

Abstract. The numerical simulations were carried out of penetration of 12.7 mm armour piercing projectile into the ARMOX 500 steel armour with the use of the AUTODYN 2D software program applying axis symmetry. The calculations were performed by means of the SPH (*Smooth Particle Hydrodynamic*) method. A constitutive Johnson-Cook model was used for both the armour and the projectile. The influence of discretization density of the numerical model on the residual velocity v_r of the projectile, its wear and time of calculations was studied. An eight times decrease in the distance between the SPH particles in the numerical model causes an over 130 fold increase of the projectile residual velocity and a 960 fold increase in the calculation time. The examined aspects included the influence of armour thickness g and yield stress R_e of the projectile material on its residual velocity and manner of the projectile and armour damage. The residual velocity of the projectile decreases together with an increase of the armour thickness and for $g = 20$ mm is $v_r = 300$ m/s. Together with a decrease of the yield stress of the projectile material its residual velocity also decreases, the wear of the projectile increases, the shape and the dimensions of cross section hole in the armour also change.
Keywords: numerical simulations, AUTODYN, SPH method, Johnson–Cook constitutive model

1. INTRODUCTION

The impact of a projectile with an armour occurs in the conditions of very high strain rates of $10^4 \div 10^7$/s [1]. The material plastic flow during its loading with high strain rates depends on its strain, the strain rate, the temperature and the material microstructure. The permanent strain produces a growth of yield stress as a result of the strain hardening. The strain rate growth also causes the material strengthening – most metals exhibit progressive growth of yield stress for the strain rates higher than 10/s [2]. The plastic strain generates heat, which is dissipated when the strain rates are low and the material remains in the isothermal conditions. In case the strain occurs violently, there is no enough time to carry the heat away and the material remains in the adiabatic conditions, what causes its thermal softening as a result of the temperature growth. There are several models for description of the behaviour of the material subjected to a load with high strain rates, for example Zerilli−Armstrong [3], Johnson−Cook [4] and its modified versions. The constitutive Johnson−Cook model expresses the equivalent tensile flow stress as a function of the plastic strain, the strain rate and the temperature as:

$$\sigma = (A + B\varepsilon^n)(1 + C \ln \dot{\varepsilon}^*)(1 - T_*^m) \tag{1}$$

where: ε − the equivalent plastic strain, $\dot{\varepsilon}^* = \dot{\varepsilon} / \dot{\varepsilon}_0$ − the dimensionless plastic strain for $\dot{\varepsilon}_0 = 1s^{-1}$, $T_* = (T - T_{300}) / (T_{melt} - T_{300})$ − the homologous temperature, T_{300} − the room temperature, T_{melt} − the melting temperature of a given material.

There are five constants in the model: A − a yield stress for strain rate $\dot{\varepsilon}_0 = 1s^{-1}$, B − a hardening constant n − a hardening exponent, C − a strain rate constant, m − a thermal softening exponent. These parameters are usually determined for large strains and high strain rates with the use of a Split-Hopkinson Pressure Bar, which enables to obtain strain rates of $\dot{\varepsilon} = 10^2 \div 10^4$/s. Higher strain rates can be obtained with the use of a Taylor impact test ($\dot{\varepsilon} = 10^4 \div 10^5$/s) or a plate-to-plate impact test ($\dot{\varepsilon} > 10^5$/s).

2. THE NUMERICAL ANALYSIS OF PENETRATION OF 12.7 MM AP PROJECTILE INTO THE STEEL ARMOUR

The numerical simulations were carried out of penetration of the 12.7 mm armour piercing projectile into the ARMOX 500 steel armour (with impact velocity of 845 m/s) with the use of AUTODYN 2D program applying axis symmetry.

The calculations were performed with the use of SPH (*Smooth Particle Hydrodynamic*) method adopting differential distances between the SPH particles, different thickness of the armour, and different values of the yield stress in the strength model of the projectile. For the latter, only the shape and dimensions of its core were taken into account. The Johnson−Cook constitutive model was used both for the projectile and the armour. As a projectile material the steel S-7 from the AUTODYN program material library was used. In the strength model the only corrected was the yield stress which value was increased to $A = 3000$ MPa. For the ARMOX 500 armour the parameters of the constitutive model were adopted on the basis of literature [5]. All the parameters of the Johnson−Cook constitutive model for both the projectile and the armour were shown in Table 1.

Table 1.   Parameters of the Johnson−Cook constitutive model for the projectile and the armour

Parameters J–C	A, MPa	B, MPa	C	n	m
Projectile	3000	477	0.012	0.18	1
Armour	849	1340	0.00541	0.0923	0.87

3. THE INFLUENCE OF DISTANCE BETWEEN THE SPH PARTICLES ON THE RESIDUAL VELOCITY OF THE PROJECTILE AND THE TIME OF CALCULATIONS

A correctly built numerical model guarantees convergence of the numerical solution w_d to the exact solution with density of model discretization (increase of number of elements n and degrees of freedom of the model N) [6]. This dependence is shown in Figure 1.
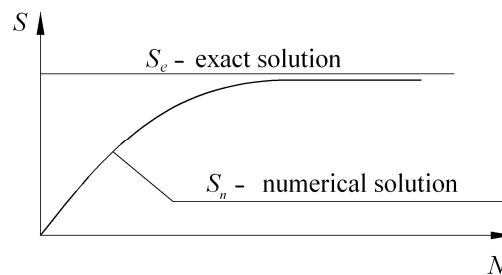

Fig. 1. Dependence of numerical solution of discrete model in function of degrees of freedom of the model N [6]

Four comparative simulations were conducted where the distance between the SPH particles was reduced by half time and time again (by increasing number of particles), while the remaining parameters were not modified.

The residual velocity v_r of the projectile, i.e. its velocity after the armour perforation, was taken as a comparative criterion.

Additionally, there were compared the mushroom diameter of the projectile D and the time of calculations t_s, in dependence of the number of particles n in the numerical model. The results were shown in Table 2 and in Figures 2 and 3.

Table 2.   Results of the numerical simulation for the variants 1÷4

Variant	Armour thickness g, mm	Distance between the SPH particles, d, mm	Number of the SPH particles in the numerical model, n	Residual velocity of the projectile, v_r, m/s	Mushroom diameter, D, mm	Time of calculations, t_s, h
1	14	0.5	15 007	4.1	15	0.1
2	14	0.25	60 051	247	12.4	1.2
3	14	0.125	240 239	439	11.2	9.3
4	14	0.0625	961 021	540	11.2	96

The residual velocity of the projectile (Fig. 2) increases together with the decrease of distance d between the SPH particles (with the increase of the SPH particles). The decrease of distance eight times ($d = 0.0625$ mm in the variant 4 with regard to $d = 0.5$ mm in the variant 1) causes the increase of the projectile residual velocity over 130 fold ($v_r = 540$ m/s in the variant 4 with regard to $v_r = 4.1$ m/s in the variant 1). It is not a proportional relationship, the residual velocity increases approaching asymptotically to the exact result (50% decrease of distance between the particles in the variant 2 with regard to the variant 1 causes the increase of the residual velocity ~60 fold with regard the increase of the residual velocity ~1.2 fold in the variant 4 with regard to the variant 3).
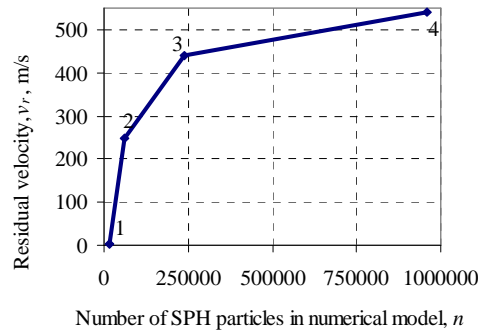

Fig. 2. Residual velocity of the projectile in function of the SPH particles number for the variants 1÷4

The decrease of distance between the SPH particles causes the decrease of the projectile mushroom diameter D (lower projectile strains).

The lowest mushroom diameter was $D = 11.2$ mm (the initial diameter of the projectile was $D = 10.9$ mm). This value was obtained using the distance between the particles $d = 0.125$ mm and the subsequent thickening of discretization of the model had no influence on this parameter (Fig. 3).
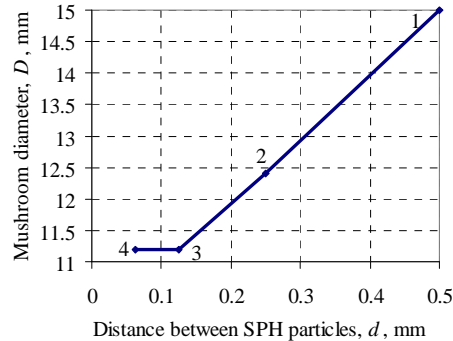

Fig. 3. Mushroom diameter D of the projectile in function of the distance d between the SPH particles for the variants 1÷4

As shown in Table 2, the time of calculations t_s prolongs together with the decrease of distance between the SPH particles, e.g. the decrease of distance by half causes prolongation of the time about 10 fold. A consecutive decrease of distance between the particles by half would prolong the time of calculations even to about 1000 h, that is why the distance in further simulations was limited to $d = 0.0625$ mm.
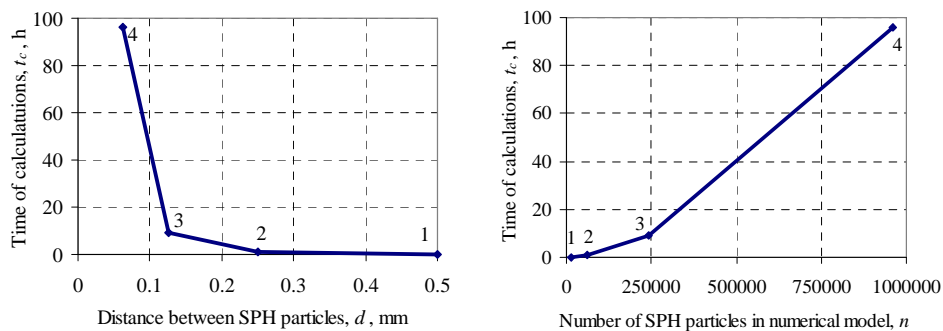

Fig. 4. Time of calculations t_s for the variants 1÷4: a – in function of distance between the SPH particles, b – in function of the SPH particles number

4. THE INFLUENCE OF THE ARMOUR THICKNESS ON THE PROJECTILE RESIDUAL VELOCITY

The specialist literature shows that the 12.7 mm armour piercing projectile B-32 perforates the RHA (*rolled homogenous armour*) of 20 mm thickness [7].

In the other work [8] it has been found that the APM2 12,7 mm projectile perforates the 20.7 mm ARMOX 500 sheet metal, when the velocity is $V_{50} = 762\pm71$ m/s. However, there is no information in the literature about the projectile residual velocity after the armour perforation.

In the following variants the thickness of the armour was increased up to 20 mm and the residual velocity in function of the armour thickness (Fig. 5) was investigated. The parameters of the projectile and armour constitutive models were the same as for the variants 1÷4 (Table 1).

Table 3. Residual velocity of the projectile for the variants 5÷10

Variant	5	6	7	8	9	10
Armour thickness, g, mm	15	16	17	18	19	20
Projectile residual velocity, v_r, m/s	504	485	452	398	343	300

The residual velocity v_r of the projectile decreases together with the increase of the armour thickness g and has approximately linear character. Following the feature, for higher armour thicknesses it can be assumed that the projectile will penetrate the armour with the thickness of 25÷26 mm.
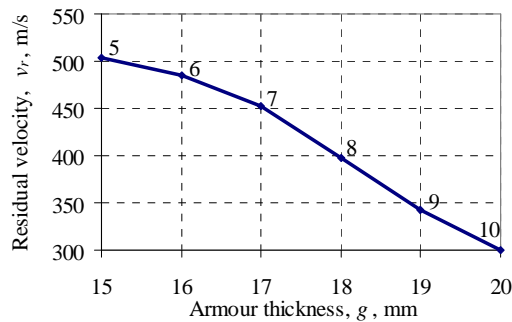

Fig. 5. The change of residual velocity of the projectile in function of the armour thickness for the variants 5÷10

5. THE INFLUENCE OF THE PROJECTILE MATERIAL YIELD STRESS ON ITS RESIDUAL VELOCITY

The influence of the projectile material yield stress R_e on its residual velocity and its wear during penetration of the 20 mm thick armour was

investigated. The yield stress was decreased to 2000 MPa and to 1539 MPa (the original value R_e for the S-7 steel) respectively.

The velocity of the projectile in the AUTODYN program can be defined as an average value from all the nodes (particles) or as a value for a given node (particle), which is representative for the projectile or its shrapnel. The projectile undergoes fragmentation and some of its elements are stopped by the armour (Table 4), together with the decrease of its material yield stress R_e.

For this reason, the residual velocity of the projectile defined as an average value from all the SPH particles would be underestimated. To avoid this, the residual velocity of the projectile for the variants 11 and 12 was defined for its centre of mass.

Together with the decrease of the material yield stress the projectile residual velocity decreases (Fig. 6). Reduction of the yield stress by almost half results with the decrease of the projectile residual velocity by about 50%. The projectile manner of damage and the shape of the hole in the armour after perforation also change (Table 4). The projectile with the material yield stress $R_e = 3000$ MPa does not undergo strains and fragmentation. The diameter of the inlet in the armour after perforation is approximately of the dimension of the cylindrical part of the projectile (its core). This dimension is constant on 0.75 length of the cross section of the hole in the armour. In the rear of the armour, this cross section of the hole increases and the outlet is of 30 mm diameter. The projectile with the material yield stress $R_e = 1539 \div 2000$ MPa undergoes plastic strains and fragmentation. The diameter of the inlet in the armour is ~18 mm (for both $R_e = 1539$ MPa and $R_e = 2000$ MPa) and its cross section increases along the whole thickness of the armour. The diameter of the outlet is of 33 mm for $R_e = 1539$ MPa and of 38 mm for $R_e = 2000$ MPa.
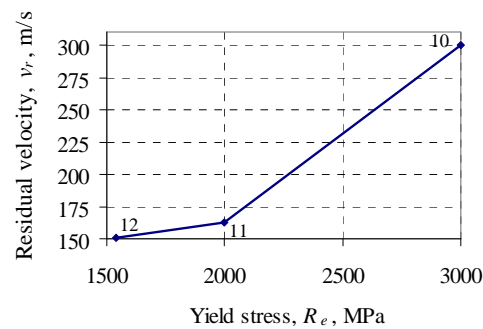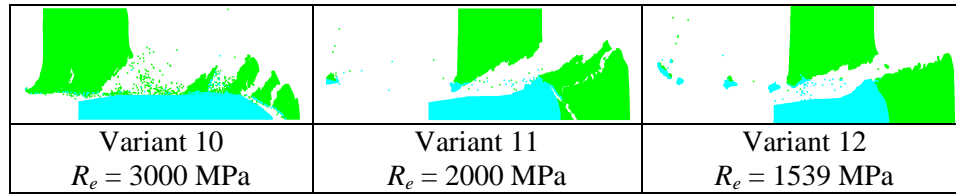

Fig. 6. The change of residual velocity v_r of the projectile in function of the projectile material yield stress for the variants $10 \div 12$

Table 4. Perforation of the 12.7 armour piercing projectile made from steel with different yield stress into the 20 mm thick ARMOX 500 steel armour − time $t = 0.15$ ms

Variant 10 $R_e = 3000$ MPa	Variant 11 $R_e = 2000$ MPa	Variant 12 $R_e = 1539$ MPa

In both these cases the projectile strikes out from the armour a so called "plug" of a truncated cone shape. The higher is the material yield stress of the projectile, the bigger is the inclination angle of element of the cone (hence the bigger diameter of the outlet in the armour after the projectile impact with $R_e = 2000$ MPa).

6. CONCLUSIONS

On the base of the conducted tests there can be drown the following conclusion:

1. Accuracy of the solution of the numerical model depends on the model discretization density. The decrease of distance between the SPH particles by 8 times results a 130 fold higher residual velocity of the projectile and a 25% smaller diameter of the projectile mushroom.

2. The residual velocity of the projectile approaches asymptotically to the exact result together with the decrease of distance between the SPH particles. Relation a of the residual velocity, e.g. for the variant 4 to the residual velocity for the variant 3 is $a = (v_{rx} = v_{r4} = 540$ m/s) / ($v_{rx-1} = v_{r3} = 439$ m/s) = 1.23 in comparison with $a = 60.25$ for the variant 2 in relation to the variant 1 (Table 5).

Table 5. Parameters of the projectile residual velocity for the variants 1÷4

Variant	Distance between the SPH particles, d, mm	Residual velocity of the projectile, v_r, m/s	Relation of the residual velocity between the following variants, $a = v_{rx}/v_{rx-1}$, for x = 2÷4
1	0.5	4.1	-
2	0.25	247	60.25
3	0.125	439	1.78
4	0.0625	540	1.23

3. The time of calculations increases together with the model discretization density. The decrease of distance between the SPH particles by 8 times prolongs the time of calculations by 960 fold.
4. An increase of the armour thickness causes a decrease of the projectile residual velocity. The change of this velocity is an approximately linear function. For the 20 mm thick armour, the residual velocity of the projectile was 300 m/s.
5. The projectile material yield stress has an influence on the projectile residual velocity (v_r = 300 m/s for R_e = 3000 MPa in comparison to v_r = 123 m/s for R_e = 1539 MPa), the projectile mushroom diameter (D = 12 mm for R_e = 3000 MPa in comparison to D = 20.6 mm) and the shape of the projectile after the armour perforation.
6. A calibration of the numerical model through selection of suitable parameters for the projectile and armour constitutive models can be facilitated by the armour firing test with the use of the high-speed camera for measurement of the projectile residual velocity and record of the projectile and the armour manner of damage.

REFERENCES

[1] Rohr I., Nahme H., Thoma K., Material characterization and constitutive modelling of ductile high strength steel for a wide range of strain rate, *International Journal of Impact Engineering*, 31, pp. 401-433, 2005.
[2] Malinowski J., Kowalewski Z., Kruszka L., *Doświadczalna metoda oraz badania plastycznego płynięcia metali w zakresie bardzo wysokich prędkości odkształcania*, Instytut Podstawowych Problemów Techniki Polskiej Akademii Nauk, Warszawa, 2007.
[3] Zerilli F.J., Armstrong R.W., Dislocation-mechanics-based constitutive relations for materials dynamics calculations, *Journal of Applied Physics* 61, pp. 1816-1825, 1987.
[4] Johnson G.R., Cook W.H., A constitutive model and data for metals subjected to large strains, Strain rates and high temperatures, *Proceedings of the Seventh International Symposium on Ballistics*, Den Haag, Netherlands, pp. 541-547, 1983.
[5] Nilsson M., *Constitutive Model for ARMOX 500T and ARMOX 600T at Low and Medium Strain Rates*, Technical Report, Swedish Defence Research Agency, 2003.

[6] Zagrajek T., Krzesiński G., Marek P., *Metoda elementów skończonych w mechanice konstrukcji*, Oficyna Wydawnicza Politechniki Warszawskiej, Warszawa, 2006.

[7] Wiśniewski A., *Pancerze − budowa, projektowanie i badanie*, Wydawnictwa Naukowo-Techniczne, Warszawa, 2001.

[8] Gooch W., Burkins M., Squillacioti R., Stockmann R. Koch, Oscarsson H., Nash C., Ballistic testing of Swedish steel ARMOX plate for U.S. armour applications, *Proceedings of the 21st International Symposium on Ballistics*, Adelaide, Australia, 19-23 April 2004.